Orbital period analyses for two cataclysmic variables: UZ Fornacis and V348 Puppis inside the period gap

Z.-B. Dai,[1,2]★ S.-B. Qian,[1,2] E. Fernández Lajús[3] and G. L. Baume[3]

[1] *National Astronomical Observatories/Yunnan Observatory, Chinese Academy of Sciences, PO Box 110, 650011 Kunming, China*
[2] *United Laboratory of Optical Astronomy, Chinese Academy of Science (ULOAC), 100012 Beijing, China*
[3] *Facultad de Ciencias Astronómicas y Geofísicas, Universidad Nacional de La Plata and Instituto de Astrofísica de La Plata
(CCT La Plata – CONICET/UNLP), Paseo del Bosque s/n, La Plata, Argentina*

ABSTRACT

Four new CCD eclipse timings of the white dwarf for polar UZ Fornacis and six updated CCD mid-eclipse times for SW-Sex-type nova-like V348 Puppis are obtained. Detailed O–C analyses are made for both cataclysmic variables (CVs) inside the period gap. Orbital period increases at a rate of $2.63(\pm 0.58) \times 10^{-11}\,\mathrm{s\,s^{-1}}$ for UZ For and $5.8(\pm 1.9) \times 10^{-12}\,\mathrm{s\,s^{-1}}$ for V348 Pup, respectively, are discovered in their new O–C diagrams. However, conservative mass transfer from the secondary to the massive white dwarf cannot explain the observed orbital period increases for both CVs, which are regarded as part of modulations at longer periods. Moreover, the O–C diagram of UZ For shows a possible cyclical change with a period of $\sim 23.4(\pm 5.1)\,\mathrm{yr}$. To explain the observed cyclical period changes in UZ For, both mechanisms of magnetic activity cycles in late-type secondaries and the light travel-time effect are regarded as probable causes. Not only does the modulation period of 23.4 yr obey the empirical correlation between P_{mod} and Ω, but also the estimated fractional period change $\Delta P/P \sim 7.3 \times 10^{-7}$ displays a behaviour similar to that of CVs below the period gap. On the other hand, a calculation for the light travel-time effect implies with a high confidence level that the tertiary component in UZ For may be a brown dwarf, when the orbital inclination of the third body is larger than $16°$.

Key words: binaries: eclipsing – stars: individual: UZ For – stars: individual: V348 Pup – novae, cataclysmic variables.

1 INTRODUCTION

A noted feature in the binary period distribution of cataclysmic variables (CVs) is the existence of a very few CVs with orbital periods between 2 and 3 h, which is the so-called 'period gap' (Katysheva & Pavlenko 2003). Several theories are proposed for interpreting this phenomenon. One of the more famous explanations (Robinson et al. 1981) is known as the interrupted-braking model, which indicates a sudden drop in the magnetic activity of the donor star when it becomes fully convective, resulting in its shrinkage within the Roche lobe and the temporarily cessation of mass transfer. Accordingly, based on the CV period gap, 'standard' evolutionary theory suggests that a CV must evolve continuously towards shorter orbital periods by losing angular momentum (Rappaport, Verbunt & Joss 1983; Spruit & Ritter 1983; King 1988).

UZ Fornacis was first detected in the *EXOSAT* archive (EXO 033319–2554.2) as a serendipitous X-ray source (Giommi et al. 1987). The subsequent optical spectroscopies, polarimetries and photometries in many different brightness states (Berriman & Smith 1988; Imamura & Steiman-Cameron 1998; Bailey & Cropper 1991) established UZ For as an eclipsing polar (or AM Her type) with a high orbital inclination ($i \approx 80°$). The high-time-resolution optical photometry operated by Perryman et al. (2001) distinctly suggests that the strong magnetic field of the white dwarf channels the accretion flow on to both of the magnetic poles of the white dwarf. However, based on the analysis of EUV and optical eclipse light curves (Bailey & Cropper 1991; Warren, Sirk & Vallerga 1995), the impacting region (accretion spot) in the lower hemisphere of the white dwarf is regarded as a major light source occulted by the mass donor star.

V348 Puppis was discovered as a faint X-ray source by the *HEAO-1* satellite (Tuohy et al. 1990). Following its spectroscopic classification, multicolour photometries detected V-shaped eclipses with large-amplitude flickering at short wavelengths. The classification of V348 Pup is disputed, since the X-ray data observed by Tuohy et al. (1990) and Rosen et al. (1994) support an intermediate-polar (or DQ Her subclass) candidate but optical

★E-mail: zhibin_Dai@ynao.ac.cn

spectra (Rodríguez-Gil et al. 2001; Froning, Long & Baptista 2003) favour a SW-Sex-type nova-like subclass identification. This means that V348 Pup in the period gap may be an important object for the study of orbital period changes.

Since the period gap is believed to be a transition zone in the evolutionary scenario, stars in the period gap can provide an opportunity to test the standard evolutionary theory of CVs. The orbital periods of UZ For and V348 Pup, which are $\sim$2.1 h and $\sim$2.4 h respectively, definitely indicate that both objects are in the period gap. Since the sharp eclipses in UZ For and V348 Pup allow the determination of eclipse timings with high precision, the variations in the orbital periods can correctly reflect their secular evolution. However, there has been no available orbital period analysis for V348 Pup until now. Regarding UZ For, Beuermann, Thomas & Schwope (1988) initially detected a decrease of the orbital period, but the following orbital period analysis (Ramsay 1994; Imamura & Steiman-Cameron 1998) concluded that its orbital period is increasing, because they missed the four times of mid-eclipse obtained by Berriman & Smith (1988). When the missed four data points and new data with high precision were added, Perryman et al. (2001) did not measure any change in the orbital period for UZ For. Therefore, the rough orbital period analysis for both CVs in previous papers fails to deduce their possible evolutionary stages.

In this paper, the updated light curves near mid-eclipse and the eclipse timings for UZ For and V348 Pup are presented in Section 2. Then Section 3 deals with the details of the O–C analysis for both CVs. Finally, discussions of the possible mechanisms for orbital period change are made in Section 4 and our principal conclusions are given in Section 5.

2 OBSERVATIONS OF ECLIPSE TIMINGS

2.1 UZ For

Four new times of light minimum are obtained from our CCD photometric observations with a Roper Scientific, Versarray 1300B camera (Princeton Instruments, Trenton, NJ, USA) with a thinned EEV CCD36-40 de 1340 × 1300 pixel CCD chip, attached to the 2.15-m Jorge Sahade telescope at Complejo Astronomico El Leoncito (CASLEO), San Juan, Argentina. The BVR photometries were carried out on 2009 November 19, and the observation in the I-filter was made on 2009 November 20. Two nearby stars that have a similar brightness in the same viewing field of the telescope are chosen as the comparison star and the check star, respectively. All images were reduced by using PHOT (to measure magnitudes for a list of stars), the aperture photometry package of IRAF. The clock of the control computer operating the VersArray 1300B CCD camera is calibrated against UTC time using the GPS receiver's clock. The estimated precision of the time-stamp associated with each CCD frame is about 0.5 s. A uniform exposure time for $BVRI$ bands of 60 s is adopted, which is approximately the time resolution of each time-series (60.48 s). During our Complejo Astronómico El Leoncito (CASLEO) observations, an estimate of the magnitude of UZ For is $V \sim 18.1$ mag, which implies that it is in a low brightness state at the time of our observations.

Inspections of Fig. 1 suggest that the eclipse depth of the white dwarf is clearly dependent on the band. Although the time resolution in our light curves is not high enough to identify the different occulted light sources in detail, the eclipse light curve in the I-filter shown in Fig. 2 may reveal an eclipse morphology similar to the descriptions in the literature (Bailey & Cropper 1991; Imamura & Steiman-Cameron 1998). The times of total eclipse and the flat-
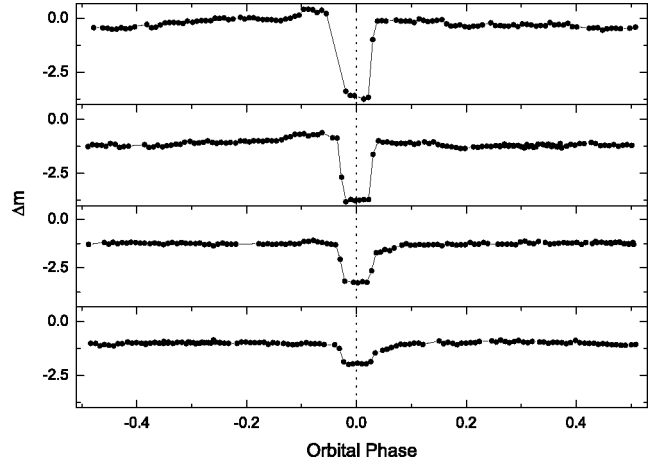

Figure 1. The light curves of polar UZ For in the $BVRI$ bands measured on 2009 November 19 and 20 using the 2.15-m Jorge Sahade telescope at CASLEO. From top to bottom, the light curves correspond to B, V, R, I bands.
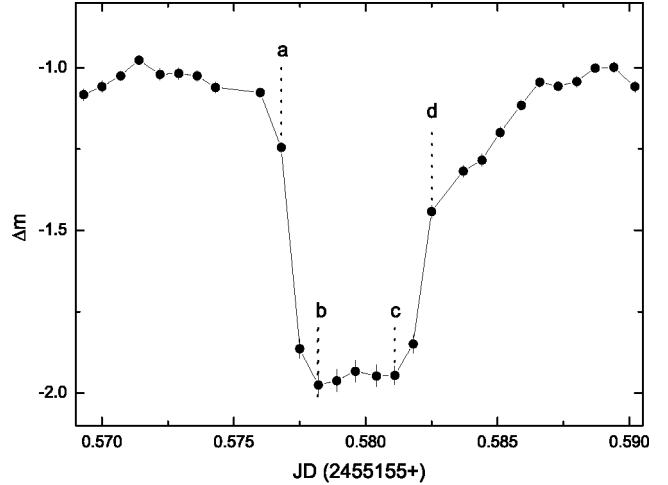

Figure 2. The eclipse part of the light curve of polar UZ For in the I band is plotted. Points a, b, c and d roughly indicate the beginning and end of ingress and egress, respectively. The approximately symmetrical profiles in the ingress and egress are clearly shown.

bottomed minima can be estimated as $t_{ad} \sim 8$ min and $t_{bc} \sim 4$ min. By using the midpoint times of steep ingress and egress of eclipse, we defined four mid-eclipse times of the primary accretion hotspot corresponding to $BVRI$ bands, respectively. Considering that the time resolution of our observations is $\sim$60 s, the quoted uncertainties are estimated as 0.0005 d. The four new eclipse timings indicate that they are wavelength-dependent, with the eclipse occurring earlier at shorter wavelengths. This clearly implies the composite eclipse of two sources, the bluer source being eclipsed earlier than the redder one. The average difference of the timings obtained at different wavelengths is about 0.0003 d. According to the eclipse phenomenology of UZ For (Bailey & Cropper 1991; Warren et al. 1995; Imamura & Steiman-Cameron 1998; Perryman et al. 2001), there is a non-negligible uncertainty associated with the transformation of hotspot mid-eclipse timings into white dwarf ones, which affects all timings except those of Bailey & Cropper (1991). Therefore, common error bars of 0.00046 d are assigned to all data in the sample other than the timings obtained by Bailey & Cropper

Table 1. The 44 eclipse timings for the polar UZ For.

JD. Hel. 240 0000+	Type	Error (d)	Method	E (cycle)	(O–C) (d)	Ref.
45567.1768700*	pri	.00046	*EXOSAT*	0	.00129	(1)
46446.9730700*	pri	.00046	*EXOSAT*	10013	.00059	(1)
47088.7418100^q	pri	.00046	ccd	17317	−.00003	(2)
47089.7082700^q	pri	.00046	ccd	17328	−.00009	(2)
47090.5870500^q	pri	.00046	ccd	17338	.00003	(2)
47091.5535000^q	pri	.00046	ccd	17349	−.00004	(2)
47094.7166200^q	pri	.00046	ccd	17385	−.00007	(2)
47097.7918200^q	pri	.00046	ccd	17420	−.00016	(2)
47127.1387000^f	pri	.00046	ccd	17754	−.00035	(3)
47127.2270000^f	pri	.00046	ccd	17755	.00008	(3)
47127.7549000^q	pri	.00046	pe	17761	.00079	(4)
47127.8431000^q	pri	.00046	pe	17762	.00109	(4)
47128.7213000^q	pri	.00046	pe	17772	.00067	(4)
47128.8089000^q	pri	.00046	pe	17773	.00041	(4)
47145.0636000^f	pri	.00046	ccd	17958	−.00001	(3)
47437.9191700*	pri	.00046	pe	21291	−.00003	(5)
47827.9541300^q	pri	.00006	ccd	25730	.00002	(6)
47828.0419900^q	pri	.00006	ccd	25731	.00002	(6)
47828.1298700^q	pri	.00006	ccd	25732	.00003	(6)
47829.0084400^q	pri	.00006	ccd	25742	−.00005	(6)
47829.0963500^q	pri	.00006	ccd	25743	−.00001	(6)
47829.1842100^q	pri	.00006	ccd	25744	−.00001	(6)
48482.7271658*	pri	.00046	ROSAT	33182	−.00028	(5)
48482.9029958*	pri	.00046	ROSAT	33184	−.00018	(5)
48483.3422558*	pri	.00046	ROSAT	33189	−.00025	(5)
48483.4301258*	pri	.00046	ROSAT	33190	−.00025	(5)
48483.6058458*	pri	.00046	ROSAT	33192	−.00026	(5)
49276.6792538^q	pri	.00046	EUVE	42218	−.00054	(7)
49310.3317728^q	pri	.00046	EUVE	42601	−.00049	(7)
49752.6467558^h	pri	.00046	pe	47635	−.00027	(8)
49753.6132158^h	pri	.00046	pe	47646	−.00033	(8)
49755.5463358^h	pri	.00046	pe	47668	−.00025	(8)
49755.6341658^h	pri	.00046	pe	47669	−.00028	(8)
50018.7032958^f	pri	.00046	pe	50663	−.00035	(8)
50020.7236358^f	pri	.00046	pe	50686	−.00092	(8)
50021.6908358^f	pri	.00046	pe	50697	−.00023	(8)
50021.7785758^f	pri	.00046	pe	50698	−.00036	(8)
51522.4319264^i	pri	.00046	STJ	67777	−.00140	(9)
51528.4067702^i	pri	.00046	STJ	67845	−.00141	(9)
51528.4946341^i	pri	.00046	STJ	67846	−.00141	(9)
55154.6168380^{Vq}	pri	.00046	ccd	109115	.00101	(10)
55154.7048690^{Rq}	pri	.00046	ccd	109116	.00121	(10)
55154.7922168^{Bq}	pri	.00046	ccd	109117	.00061	(10)
55155.5835680^{Iq}	pri	.00046	ccd	109126	.00121	(10)

Notes. *the unknown state; ^{q}the low state; ^{f}the faint high state; ^{i}the intermediate state; ^{h}the high state; ^{BVRI}the observed bands.

References: (1) Osborne et al. (1988); (2) Beuermann et al. (1988); (3) Ferrario et al. (1989); (4) Berriman & Smith (1988); (5) Ramsay (1994); (6) Bailey & Cropper (1991); (7) Warren et al. (1995); (8) Imamura & Steiman-Cameron (1998); (9) Perryman et al. (2001); (10) this paper.

(1991). Moreover, in order to apply the uniform time system, the three eclipse timings in TDB observed by Perryman et al. (2001) and our new data in UTC are transformed to HJD. All 44 times of light minimum from 1983–2009 for UZ For, including four new data from our observation, are listed in Table 1.

2.2 V348 Pup

V348 Pup was observed over four nights using the 0.6-m Helen Sawyer Hogg (HSH) telescope at Complejo Astronomico

El Leoncito (CASLEO), San Juan, Argentina. The first three observations on 2008 November 28 and 2009 January 14 and 16 were obtained with a Photometric CH250 PM512 CCD camera (Photometrics, Tucson, AZ, USA). The final observation on 2009 November 24 was obtained with an Apogee Alta U8300 Kodak KAF8300 chip (Apogee Imaging Systems, Roseville, CA, USA). All CCD photometries were unfiltered. A nearby star that has a similar brightness in the same viewing field of the telescope is chosen as the comparison star. All measurements have been corrected for differential extinction. For all four nights, the estimated magnitude of V348 Pup
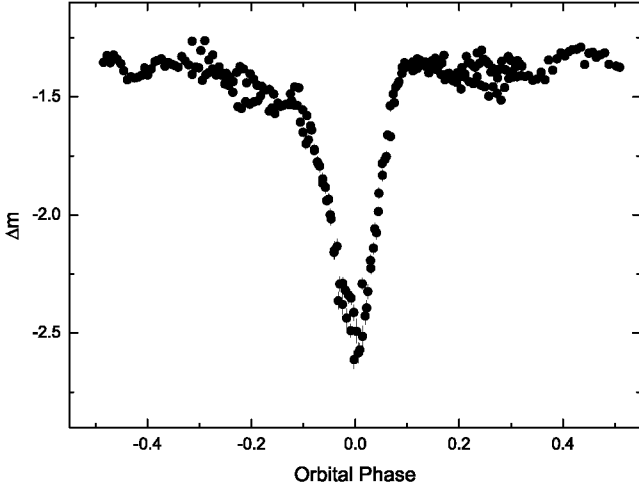
Figure 3. The unfiltered light curve of V348 Pup observed on 2008 November 28 using the 0.6-m Helen Sawyer Hogg (HSH) telescope at CASLEO is plotted. A V-shaped eclipse profile with probable time resolution is distinctly identifiable.

is $V \sim 15$ mag, which is similar to the photometries (Rolfe, Haswell & Patterson 2000). Moreover, the V-shaped eclipse of V348 Pup is clearly shown in Fig. 3 as expected from the literature (e.g. Rolfe et al. 2000; Rodríguez-Gil et al. 2001). This implies that the nova-like V348 Pup may be a stable CV that is totally different from the polar UZ For. The calibrated clock used in observations is the same as that of UZ For. The exposure times for the observations on 2008 November 28, 2009 January 14 and 16 and 2009 November 24 were 60, 30, 25 and 60 s, respectively. Since the mid-eclipse of V348 Pup is V-shaped, different from that of UZ For, six mid-eclipse timings were derived using a parabolic fitting method to the deepest part of the eclipse. The uncertainties of the mid-eclipse timings in our observations are estimated to be ~ 0.0005 d. Including the previous 48 times of light minimum for V348 Pup (Tuohy et al. 1990; Rolfe et al. 2000), we listed all 54 available times of light minimum covering about 21 yr in Table 2.

3 ANALYSES OF ORBITAL PERIOD CHANGE

3.1 UZ For

The updated linear ephemeris in HJD (Warren et al. 1995) is used to calculate the O–C values of 44 eclipse timings and, after linear revision, the new epochs and average orbital period of UZ For were derived as

$$T_{\min} = \text{HJD } 244\,5567.175\,678(67) + 0.087\,865\,4654(23)E, \quad (1)$$

with a standard deviation $\sigma_1 = 6.4 \times 10^{-4}$ d. The new calculated O–C values are listed in column 6 of Table 1. The new O–C diagram for UZ For shown in Fig. 4 implies a possible departure in the orbital period of UZ For. However, a simple sinusoidal or quadratic fit cannot completely describe the variations in the upper panel of Fig. 4. Therefore we attempted to use a quadratic-plus-sinusoidal ephemeris to fit the O–C values and the least-squares solution for the O–C diagram of UZ For leads to

$$(O\text{–}C)_1 = 2.35(\pm 0.65) \times 10^{-3} - 1.34(\pm 0.31) \times 10^{-7}E$$
$$+ 1.16(\pm 0.25) \times 10^{-12}E^2$$
$$+ 1.01(\pm 0.34) \times 10^{-3} \sin[0°0037(\pm 0°0008)E$$
$$+ 283°9(\pm 8°8)], \quad (2)$$

with standard deviation $\sigma_2 = 2.8 \times 10^{-4}$ d. Although the data near 17 000 cycles present large scatter due to the early four data derived from light curves with very low time resolution (Berriman & Smith 1988), the reduced χ^2 of equation (2) is calculated to be ~ 0.43, which is lower than unity. Moreover, the data points shown in Fig. 4 clearly indicate that a cyclical period variation with a period of $23.4(\pm 5.1)$ yr superimposed on a secular orbital period increase is significant. However, the small quadratic term in equation (2) implies that the quadratic ingredient in the O–C diagram of UZ For may be not significant. A linear-plus-sinusoidal ephemeris with the same modulation period as that in equation (2) is estimated to be

$$(O\text{–}C)_1 = -4.8(\pm 1.8) \times 10^{-4} + 5.9(\pm 2.8) \times 10^{-9}E$$
$$+ 6.5(\pm 1.2) \times 10^{-4} \sin[0°0037(\pm 0°0008)E$$
$$+ 52°8(\pm 11°0)], \quad (3)$$

with standard deviation $\sigma_3 = 4.4 \times 10^{-4}$ d. Fig. 5 suggests that the best-fitting sinusoidal period for equation (3) may be larger than 23 yr. Thus, we allowed the sinusoidal period to be one of the free parameters of the fit. However, since the data points for UZ For only cover about half of a whole sinusoid period, we cannot find a best fit with a sinusoid period about twice the baseline of the current data. Accordingly, the further data points of UZ For are important for obtaining a precise linear-plus-sinusoidal ephemeris. In order to describe the significant level of the quadratic term in equation (2), a F-test as described by Pringle (1975) is attempted to assess the significance of the quadratic terms in equation (2). The parameter λ is denoted as

$$\lambda = \frac{\sigma_3^2 - \sigma_2^2}{\sigma_2^2/(n-6)}, \quad (4)$$

where n is the number of data points. Thus, a calculation gives $F(1, 38) = 55.8$, which suggests that it is significant well above the 99.99 per cent level. According to equation (2), the orbital period increase rate of UZ For, $\dot{P}$, can be calculated to be $2.63(\pm 0.58) \times 10^{-11}$ s s^{-1}, which is similar to the previous works (Ramsay 1994; Imamura & Steiman-Cameron 1998).

3.2 V348 Pup

The recent ephemeris derived by Rodríguez-Gil et al. (2001) is used to calculate the O–C values of 54 eclipse timings for V348 Pup. Since the investigation of Fig. 6 suggests larger scatter during the observation season than the error of each data point, we assumed a common error bar ~ 0.0003 d for obtaining a fit with unity reduced χ^2. The O–C diagram shown in Fig. 6 clearly implies an orbital period increase. Therefore, a quadratic ephemeris for V348 Pup can be calculated to be

$$\text{Min } I = 244\,8591.667\,94(4) + 0.101\,838\,934(6)E$$
$$+ 2.94(\pm 0.98) \times 10^{-13}E^2, \quad (5)$$

with reduced $\chi^2 \sim 1.2$. Although the large scatter in the O–C diagram prevents further analysis of the orbital period changes in V348 Pup at present, the observations over a longer baseline may be capable of detecting a cyclical variation with a large period. The orbital period increase rate of V348 Pup, $\dot{P}$, can be estimated to be $5.8(\pm 1.9) \times 10^{-12}$ s s^{-1}. Although the large scatter in observation seasons affects the uncertainty of $\dot{P}$, the average O–C diagram of V348 Pup produced by averaging the mid-eclipse timings during each observation season strongly suggests an orbital period increase for V348 Pup. Moreover, an F-test is used to assess the significance of the quadratic term in equation (5). The parameter $\lambda = 5.8$ indicates that it is significant with ~ 99 per cent level.

Table 2. The 54 eclipse timings for the SW-Sex-type nova-like V348 Pup.

JD. Hel. 2400000+	Type	Error (d)	Method	E (cycle)	(O–C) (d)	Ref.
47210.121125	pri	.0003	pe	−13566	.00009	(1)
47211.954000	pri	.0003	pe	−13548	−.00013	(1)
47212.055875	pri	.0003	pe	−13547	−.00010	(1)
47212.157708	pri	.0003	pe	−13546	−.00010	(1)
47213.990625	pri	.0003	pe	−13528	−.00029	(1)
47240.061917	pri	.0003	pe	−13272	.00024	(1)
48591.769462	pri	.0003	ccd	1	−.00035	(2)
48592.686379	pri	.0003	ccd	10	.00002	(2)
48593.705382	pri	.0003	ccd	20	.00063	(2)
48593.806642	pri	.0003	ccd	21	.00006	(2)
48594.722715	pri	.0003	ccd	30	−.00042	(2)
48594.824510	pri	.0003	ccd	31	−.00047	(2)
48595.640158	pri	.0003	ccd	39	.00047	(2)
48595.742287	pri	.0003	ccd	40	.00076	(2)
48596.657488	pri	.0003	ccd	49	−.00059	(2)
48596.759320	pri	.0003	ccd	50	−.00060	(2)
48597.676629	pri	.0003	ccd	59	.00016	(2)
48597.778677	pri	.0003	ccd	60	.00037	(2)
48598.694383	pri	.0003	ccd	69	−.00047	(2)
48598.796652	pri	.0003	ccd	70	−.00004	(2)
49020.613001	pri	.0003	ccd	4212	−.00055	(2)
49020.715111	pri	.0003	ccd	4213	−.00027	(2)
49021.632451	pri	.0003	ccd	4222	.00052	(2)
49021.734218	pri	.0003	ccd	4223	.00044	(2)
49022.650034	pri	.0003	ccd	4232	−.00029	(2)
49022.752227	pri	.0003	ccd	4233	.00006	(2)
49027.640565	pri	.0003	ccd	4281	.00013	(2)
49029.779356	pri	.0003	ccd	4302	.00031	(2)
49030.695522	pri	.0003	ccd	4311	−.00008	(2)
49030.797304	pri	.0003	ccd	4312	−.00014	(2)
49031.612099	pri	.0003	ccd	4320	−.00005	(2)
49031.714122	pri	.0003	ccd	4321	.00013	(2)
49032.630438	pri	.0003	ccd	4330	−.00010	(2)
49032.732446	pri	.0003	ccd	4331	.00007	(2)
49039.657734	pri	.0003	ccd	4399	.00031	(2)
49039.759941	pri	.0003	ccd	4400	.00068	(2)
49040.573722	pri	.0003	ccd	4408	−.00025	(2)
49040.675596	pri	.0003	ccd	4409	−.00022	(2)
49041.592531	pri	.0003	ccd	4418	.00016	(2)
49720.653953	pri	.0003	ccd	11086	−.00041	(2)
49720.756257	pri	.0003	ccd	11087	.00006	(2)
49721.571129	pri	.0003	ccd	11095	.00022	(2)
49721.672783	pri	.0003	ccd	11096	.00004	(2)
49722.589171	pri	.0003	ccd	11105	−.00013	(2)
49722.690736	pri	.0003	ccd	11106	−.00040	(2)
49723.607919	pri	.0003	ccd	11115	.00023	(2)
49723.709706	pri	.0003	ccd	11116	.00018	(2)
49723.811139	pri	.0003	ccd	11117	−.00023	(2)
54798.649900	pri	.0003	ccd	60949	.00093	(3)
54798.752050	pri	.0003	ccd	60950	.00120	(3)
54800.686720	pri	.0003	ccd	60969	.00097	(3)
54845.598410	pri	.0003	ccd	61410	.00170	(3)
54847.635140	pri	.0003	ccd	61430	.00160	(3)
55159.771100	pri	.0003	ccd	64495	.00130	(3)

References: (1) Tuohy et al. (1990); (2) Rolfe et al. (2000); (3) this paper.

4 DISCUSSION

4.1 Secular orbital period increase

Normal mass transfer for both binaries from the red dwarf to the white dwarf is expected, since hotspots on the surface of the white dwarf and occasional X-ray and UV flaring in UZ For are observed (e.g. Bailey & Cropper 1991; Warren et al. 1995; Imamura & Steiman-Cameron 1998; Perryman et al. 2001; Pandel & Córdova 2002), and the identification of V348 Pup as a SW-Sex-type system with an enhanced mass transfer rate is confirmed in Rodríguez-Gil et al. (2001) and Froning et al. (2003). Accordingly, the orbital
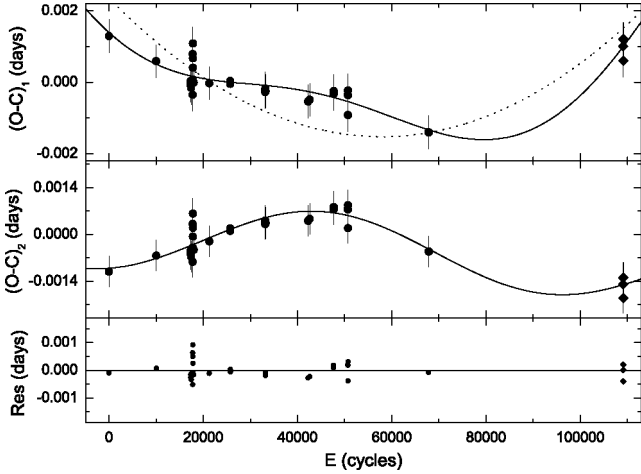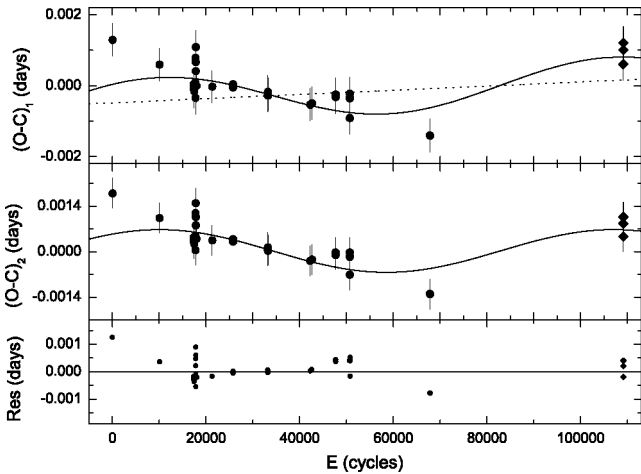
Figure 4. The $(O–C)_1$ values of UZ For are fitted in the top panel with the ephemeris displayed in equation (2). After removing the quadratic element from the $(O–C)_1$ diagram, the $(O–C)_2$ values plotted in the middle panel strongly suggest a cyclical period change with a low amplitude. The residuals and their linear fitted solid line are presented in the bottom panel. The solid circles and diamonds in the three panels denote the data compiled from previous papers and those we observed, respectively.

Figure 5. The $(O–C)_1$ values of UZ For are fitted in the top panel with the ephemeris displayed in equation (3). After removing the linear element from the $(O–C)_1$ diagram, the middle panel strongly indicates a large departure from the fitted curve. The symbols are the same as in Fig. 4.

period increase in both CVs should be predicted in principle. However, considering that the conservative mass transfer from a less massive star to a more massive one in a binary with increasing orbital period and separation is sustainable if the mass-donor star expands faster than its Roche lobe, conservative mass transfer for both CVs is not a plausible explanation for the observed secular orbital period increase. The physical parameters of both CVs deduced by modelling the eclipse light curves for UZ For (Bailey & Cropper 1991; Imamura & Steiman-Cameron 1998) and by measuring the radial velocity curves for V348 Pup (Rodríguez-Gil et al. 2001), respectively, indicate that both secondaries are low-mass main-sequence stars without violent expansion and the mass ratios of the secondary star to the white dwarf are less than unity. By using the system parameters of both CVs and the derived orbital period increase rates, we estimated the expansion rate of the Roche lobe of the secondary star, $\dot{R}_{r12}$ caused by mass transfer in the case of con-
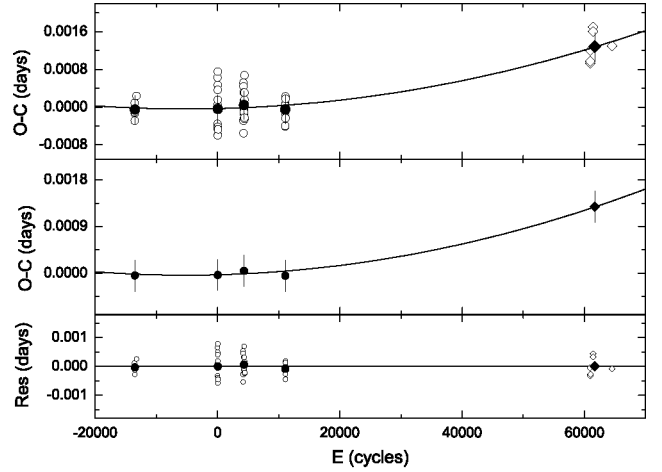

Figure 6. The O–C diagrams of V348 Pup are fitted by the quadratic ephemeris in equation (5). The open and solid symbols refer to the individual timings and the average ones, respectively. The residuals and their linear fitted solid line are presented in the bottom panel. Data from the literature and our observations are denoted by circles and diamonds, respectively.

servation to be $\sim 1.1 \times 10^{-8}\,R_\odot\,yr^{-1}$ and $\sim 2.5 \times 10^{-9}\,R_\odot\,yr^{-1}$ for UZ For and V348 Pup, respectively. Moreover, the calculated conservative mass transfer for both CVs may be adiabatic mass transfer, since the mass-loss time-scales for both secondaries are lower than their Kelvin–Helmholtz time-scales. According to the results calculated in polytropic models, a low-mass main-sequence star as mass-donor star in a binary with a rapid mass transfer (i.e. adiabatic mass transfer) may expand with an exponent $\sim 1/3$ (Hjellming & Webbink 1987). Thus, the possible expansion rates of the mass-donor stars $\dot{R}_2$ can be estimated to be $2.9 \times 10^{-9}\,R_\odot\,yr^{-1}$ and $7.8 \times 10^{-10}\,R_\odot\,yr^{-1}$ for UZ For and V348 Pup, respectively, a factor of ~ 3 less than the respective $\dot{R}_{r12}$. This paradox may imply that both CVs in the period gap are interesting objects and worthy of further observations to investigate their secular orbital period variations. On the other hand, since current data with large scatter for both CVs limit the precise detection of secular orbital period increases, the possibility that the observed increase trend in the O–C diagram may reflect part of another modulation on a longer time-scale cannot totally be ruled out.

4.2 A cyclical period variation in UZ For

A notable cyclical period variation with a period of $\sim 23.4(\pm 5.1)\,yr$ is presented in the middle panel of Fig. 4 after removing the quadratic element. However, the fact that there is only one cycle of the modulation and the large scatter shown in Fig. 4 suggest that it is yet not possible to judge whether the modulation is strictly periodic or not. Since the spectral type of the secondary of UZ For is regarded as an M4–M5 dwarf (Ferrario et al. 1989; Pandel & Córdova 2002), a solar-type magnetic activity cycle in its convective shell should be considered to explain the observed oscillations in the O–C diagram (Hall 1989; Applegate 1992; Lanza 2006). According to the regression relationship between the length of the modulation period P_{mod} and the angular velocity Ω derived by Lanza & Rodonò (1999),

$$\log P_{mod} = -0.36(\pm 0.10)\log \Omega + 0.018, \tag{6}$$

a slope ~ -0.43 for UZ For can be estimated. This suggests that UZ For can fit the relationship well. Furthermore, according to equation (2), the fractional period change $\Delta P/P$ for UZ For can be

estimated to be $\sim 7.3 \times 10^{-7}$. Since the orbital period of UZ For is about 2.1 h, which is inside the period gap, the $\Delta P/P$ value of UZ For can offer a good sample with which to check the diagram of $\Delta P/P$ versus Ω of the active component star for CVs (Borges et al. 2008). A calculation indicates that UZ For obviously deviates from the relation $\Delta P/P \propto \Omega^{-0.7}$ and displays a behaviour similar to that of the CVs below the period gap (Borges et al. 2008). However, considering that the generation of large-scale magnetic fields in fully convective stars may be different from that of stars with radiative cores (Dobler 2005), magnetic activity cycles may still provide a possible explanation for UZ For. On the other hand, using an extended model with Applegate's considerations introduced by Lanza (2005, 2006), the longest time-scale of energy dissipation $\tau \approx 0.8$ yr for the magnetic active cycles in UZ For can be estimated from the eigenvalue of the equation of angular momentum conservation, $\lambda_{20} \approx 3.95 \times 10^{-8}$ s^{-1}. Moreover, the scaling relationship of the dissipated power and the luminosity of the secondary stars derived by Lanza & Rodonò (2006) suggests that the required energy cannot be sustained by the stellar luminosity of UZ For. This means that a reconsideration of the hypothesis of magnetic active cycles is needed to interpret the observed cyclical period variations in CVs.

Another plausible mechanism for the cyclical period variation is the light travel-time effect, which is caused by a perturbation from a tertiary component. An inspection of Fig. 4 suggests that the orbital eccentricity of the third star is near zero. By using the amplitude of the sinusoidal curve and Kepler's Third Law, the projected distance $a' \sin(i)$ from the binary to the mass centre of the triple system and the mass function of the third component $f(m_3)$ can be calculated to be $0.17(\pm 0.06)$ au and $9.4(\pm 0.9) \times 10^{-6}$ M$_\odot$, respectively. We set a combined mass of 0.7 M$_\odot$ + 0.14 M$_\odot$ for the eclipsing pair of UZ For. If the orbital inclination of the third component in this system is large than 16°, it may be a brown dwarf with a confidence level ≥ 82 per cent based on the inclination. According to the both relationships described in Fig. 7, the mass of the third star in UZ For is close to the lower limit of a brown dwarf's mass, ~ 0.014 M$_\odot$ (Chabrier & Baraffe 2000; Burrow et al. 2001), as long as the inclination of the third star is higher than 85° and the distance from the third body to the mass centre of system is ~ 7.6 au, which is over three orders of magnitude larger than the binary separation e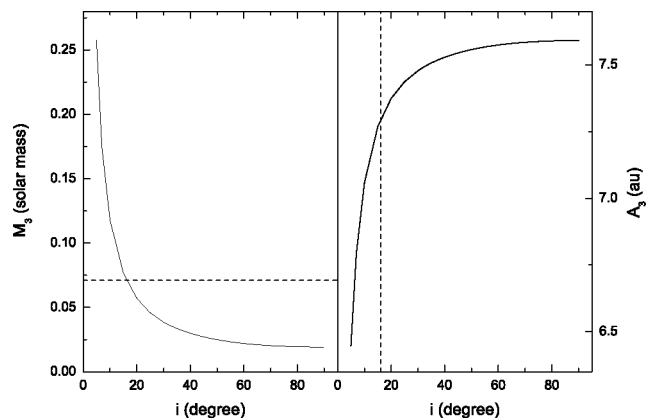stimated from the orbital period of UZ For. Thus, this third star can survive the previous common envelope evolution of the parent binary. Moreover, the mass of this third star implies that it may be a critical substellar object between brown dwarf and giant planet.

5 CONCLUSION

The orbital period variations in two CVs with deep eclipse inside the period gap, UZ For and V348 Pup, are investigated in detail. The new eclipse timings, comprising four data points for polar UZ For and six data points for V348 Pup, respectively, suggest that orbital period increases with a rate $2.63(\pm 0.58) \times 10^{-11}$ s s^{-1} for UZ For and $5.8(\pm 1.9) \times 10^{-12}$ s s^{-1} for V348 Pup, respectively, are observed in the O–C diagrams. However, based on the physical parameters of both CVs, the observed secular orbital period increase shown in Figs 4 and 6 cannot be explained by conservative mass transfer, since $\dot{R}_{rl2} > \dot{R}_2$ in the case of conservation for both CVs. Thus, the increasing trend shown in the O–C diagrams for both CVs may be just part of another modulation at a longer period. Moreover, the failure of a linear-plus-sinusoidal ephemeris for UZ For may imply that current data in the O–C diagram only cover a half-cycle modulation.

Aside from the observed orbital period increase in both CVs, a cyclical period variation with a low amplitude of $1.01(\pm 0.34) \times 10^{-3}$ d and a period of $23.4(\pm 5.1)$ yr in UZ For is discovered. Both mechanisms of magnetic activity cycles and the light-travel effect can apparently be used to interpret the observed O–C oscillation. Regarding the former, the modulation period fits the regression relationship derived by Lanza & Rodonò (1999), and the derived fractional period change $\Delta P/P \sim 7.3 \times 10^{-7}$ displays a behaviour similar to that of CVs below the period gap in the diagram of $\Delta P/P$ versus Ω (Borges et al. 2008). Moreover, since the longest time-scale of energy dissipation $\tau \approx 0.8$ yr estimated by an extended model with Applegate's hypothesis introduced by Lanza (2005, 2006) does not support Applegate's mechanism for interpreting the observed modulation in UZ For, a new available model of magnetic active cycles is expected. On the other hand, a calculation of the light travel-time effect indicates that a brown dwarf as the third component in a 0.7 M$_\odot$ + 0.14 M$_\odot$ eclipsing pair for UZ For is possible with a confidence level ≥ 82 per cent. Assuming the inclination of the tertiary component is high, the third star may be a critical substellar object between brown dwarf and giant planet. It is important to note that uncertainties in the system parameters of both binaries affect the precision of the detailed O–C analysis for both CVs in the period gap, and extending the observational base line to check all the hypotheses discussed above is required for a more comprehensive investigation of their orbital period changes.

Figure 7. The masses and separation of the third component in UZ For for different orbital inclination i are plotted in the left and right panels, respectively. The dashed lines in the left and right panels denote a lower limit of mass of a star with hydrogen burning and the corresponding orbital inclination $i \sim 16°$, respectively.

REFERENCES

Applegate J. H., 1992, ApJ, 385, 621

Bailey J., Cropper M., 1991, MNRAS, 253, 27

Berriman G., Smith P. S., 1988, ApJ, 329, L97

Beuermann K., Thomas H. C., Schwope A., 1988, A&A, 195, L15

Borges B. W., Baptista R., Papadimitriou C., Giamakis O., 2008, A&A, 480, 481

Burrow A., Hubbard W. B., Lunine J. I., Liebert J., 2001, Rev. Mod. Phys., 73, 719

Chabrier G., Baraffe I., 2000, ARA&A, 38, 337

Dobler W., 2005, Astron. Nachr., 326, 254

Ferrario L., Wickramasinghe D. T., Bailey J., Tuohy I. R., Hough J. H., 1989, ApJ, 337, 832

Froning C. S., Long K. S., Baptista R., 2003, AJ, 126, 964

Giommi P., Angelini L., Osborne J., Stella L., Tagliaferri G., Beuermann K., Thomas H.-C., 1987, IAU Circ. 4486

Hall D. S., 1989, Sov. Sci. Rev., 50, 219

Hjellming M. S., Webbink R. F., 1987, ApJ, 318, 794

Imamura J. N., Steiman-Cameron T. Y., 1998, ApJ, 501, 830

Katysheva N. A., Pavlenko E. P., 2003, Astrophys., 46, 114

King A. R., 1988, QJRAS, 29, 1

Lanza A. F., 2005, MNRAS, 364, 238

Lanza A. F., 2006, MNRAS, 369, 1779

Lanza A. F., Rodonò, 1999, A&A, 349, 887

Osborne J. P., Giommi P., Angelini L., Tagliaferri G., Stella L., 1998, ApJ, 328, L45

Pandel D., Córdova F. A., 2002, MNRAS, 336, 1049

Perryman M. A. C., Cropper M., Ramsay G., Favata F., Peacock A., Rando N., Reynolds A., 2001, MNRAS, 324, 899

Pringle J. E., 1975, MNRAS, 170, 633

Ramsay G., 1994, Int. Bull. Variable Stars, 4075, 1

Rappaport S. V., Verbunt F., Joss P. C., 1983, ApJ, 275, 713

Robinson E. L., Barker E. S., Cochran A. L., Cochran W. D., Nather R. E., 1981, ApJ, 251, 611

Rodríguez-Gil P., Martínez-Pais I. G., Casanes J., Villada M., van Zyl L., 2001, MNRAS, 328, 903

Rolfe D. J., Haswell C. A., Patterson J., 2000, MNRAS, 317, 759

Rosen S. R., Clayton K. L., Osborne J. P., McGale P. A., 1994, MNRAS, 269, 913

Spruit H. C., Ritter H., 1983, A&A, 124, 267

Tuohy I. R., Remillard R. A., Bradt H. V., Brissenden R. J. V., 1990, ApJ, 359, 204

Warren J. K., Sirk M. M., Vallerga J. V., 1995, ApJ, 445, 909

This paper has been typeset from a TEX/LATEX file prepared by the author.